BAM Bundesanstalt fur"
Materialforschung und -prüfung

SYNTHESIS REPORT

Contract N°: BRE2 - CT92 -0176

Project N*: BE5216

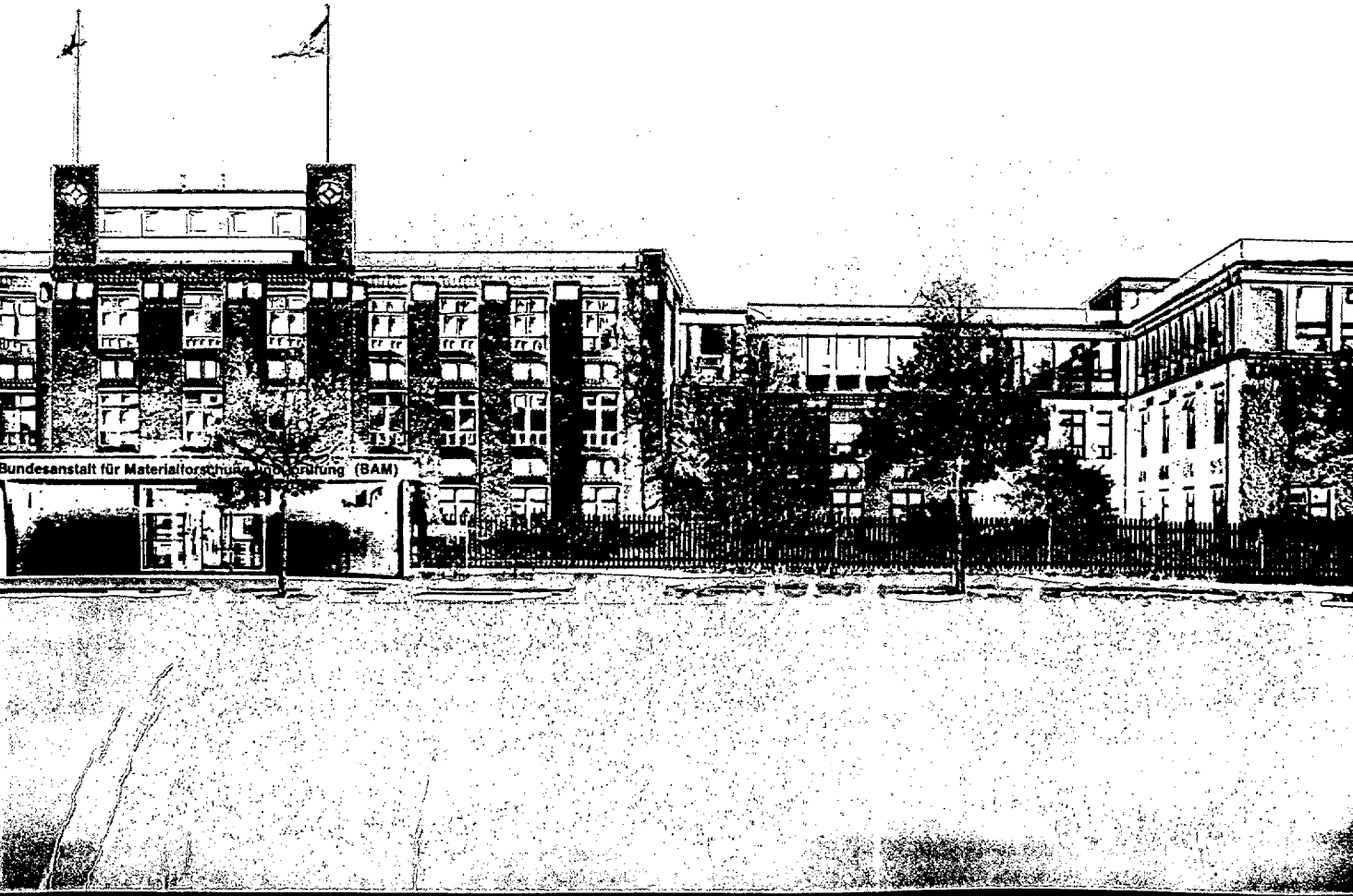

SYNTHESIS REPORT

FOR PUBLICATION

CONTRACT N°: BRE2 - CT92 -0176

PROJECT No: BE 5216

TITLE: DEVELOPMENT OF MICROSTRUCTURAL BASED VISCOPLASTIC MODELS FOR AN ADVANCED DESIGN OF SINGLE CRYSTAL HOT SECTION COMPONENTS

PROJECT COORDINATOR: J. Olschewski
Bundesanstalt für Materialforschung und -prüfung (BAM)
Laboratory V.31
Unter den Eichen 87
D-12200 Berlin

PARTNERS: BAM, Berlin (Germany)
ONERA, Chatillon (France)
ENSMP, Evry (France)
IMMG, Pendeli (Greece)

REFERENCE PERIOD FROM OL1O.1992 to 31.09.1995

STARTING DATE: 01.10.1992 **DURATION: 36 MONTHS**

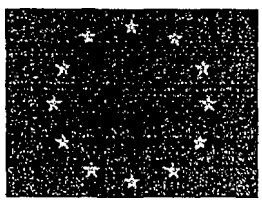

PROJECT FUNDED BY THE EUROPEAN COMMUNITY UNDER THE BRITE/EURAM PROGRAMME

Development of Microstructure Based Viscoplastic Models for an Advanced Design of Single Crystal Hot Section Components

J. Olschewski[1], G. Cailletaud[3], W. Dreyer[1], S. Forest[3], H. Klingelhöffer[1], P. Michelis[4], D. Nouailhas[2], M. Toulios[4]

1) Bundesanstalt für Materialforschung und -prüfung (BAM), Berlin, FRG
2) Office National d'Etudes et de Recherche Aérospatiales (ONERA), Châtillon, France
3) Centre des Matériaux de Ecole Nationale Superieure des Mines de Paris, Evry, France
4) Institute of Mechanics of Materials& Geostructures S. A., Pendeli, Greece

This paper summarizes the research activities of the research project BE5216 within the BriteEuRam programme. The results developed include: constitutive models taking into account the heterogeneity of the deformation of two-phase single crystalline super-alloys on two levels, advanced experimental testing device for internal pressure testing, improved high-temperature measurement methods for local strain fields.

Two single crystal superalloys, SC16 and MC2, were investigated. Both alloys have shown a heterogeneous deformation pattern at low temperatures due to shear band formation on a macro-level and an evolving γ - γ' - microstructure on a micro-level resulting in high internal stresses and a changing global anisotropy of the material. The models and advanced inelastic analysis methods were developed to describe these material phenomena. Supported was the model development by multiaxial mechanical testing and accompanying microstructural investigations.

This report discusses the design of a laboratory prototype testing machine which is capable of subjecting thin tubular specimens to cyclic torsion and/or to a constant internal pressure at temperatures reaching 1050° C. In addition, due to the 'safe' use of borosilicate glasses as the pressure transmitting medium, it offers new possibilities for local strain measurement using a long distance microscope and image analysis techniques. These developments in experimental techniques have been applied to the testing of the SC alloy MC2 in the temperature range of 850-1050 **°C.**

1. Introduction

Single crystal (SC) alloys are being increasingly used in aero-engine and industrial gas turbine applications in order to increase their operating temperatures. The development of new high temperature gas turbine alloys has changed the sector of application of ground engines to that of combined cycle plants for base power production. With turbine inlet temperatures, which can be endured by single crystal turbine blades, the net efficiency of combined cycle plants cart be increased to more than 50%. This in turn will reduce the emission of CO_2 considerably. Beside major environmental effects which are demanded by the public, increasing efficiencies result in a reduced consumption of fossile fuel and in savings of scarce materials.

Hot section components of both aircraft and land based gas turbine engines are subjected to severe cyclic thermal-mechanical loading conditions during the engine service. It is therefore crucial for the design of the critical parts of gas turbines to predict the response of the alloy to these loads correctly. A comprehensive understanding of the material at these extremes of temperature and strain is necessary to develop reliable constitutive models and failure criteria. It

is the need for improved engine performance that will spur development of advanced analytical tools and expanded experimental capabilities [1]. To improve engine reliability and durability is also an important economical factor because of tremendous maintainance costs.

In engineering practice, the design of hot section components is based on thermo-mechanical analyses of the most critical parts. An assessment of the maximum inelastic strain in these parts is made on assumptions valid for isotropic materials. Materials used in today's turbine engine hot section components are operating under conditions (temperature, mechanical loads) where time-independent (plastic] and time-dependent (creep) material phenomena occur simultaneous] y and where the inelastic material behaviour is strongly crystal orientation dependent. Therefore, in order to achieve the demand for improved life assessment rules, methodologies are needed which are based on inelastic analysis taking the anisotropy of single crystal alloys and the heterogeneity of the deformation in two-phased superalloy into account.

The viscoplastic constitutive models developed so far for single crystals [2 -6] have neglected the heterogeneity of the material. On a macroscale, shear bands appear in laboratory specimens at low temperatures. This leads to misinterpretations of the real material response when the results from laboratory specimens are transferred to components. On a microscale, two phases, y'- precipitates embedded coherently in a y- matrix, are present which do not deform uniforml y. In addition, the lattice mismatch between the two phases causes considerable internal (misfit) stresses which interact with the macroscopic stresses produced by the thermo-mechanical loading. The problem of heterogeneity becomes more crucial if the changing y-y 'morphology under operating conditions is considered [7]. The y-y' - morphology of a real component does not correspond in general to the microstructure studied in laboratories.

Therefore, the main objective of the present project was to develop constitutive models which account for the heterogeneity of the materials and to upgrade the experimental techniques for anisotropic materials in the high temperature regime.

The development and validation of material models and failure criteria for (SC) alloys however requires testing under biaxial loadings, in addition to the standard uniaxial testing along selected crystallographic orientations. Moreover due to the an isotropic behaviour of these alloys it is necessary to measure the deformation locally. This report discusses two main developments in experimental mechanics which are aimed to contribute to these two requirements. The first concerns the design of a cyclic torsion-internal pressure testing machine which uses glass as a pressure transmitting medium in order to allow the visual observation of the specimen surface without the risk of injuries when it ruptures. The second development concerns the use of a long distance microscope and image capturing/processing system which tracks the movement of grids of markers placed on the specimen surface in order to determine the anisotropic deformation. Finally the application of these techniques to the testing of the SC superalloy MC2 in the temperature range 850- 1050°C is discussed.

The society demand for the provision of sufficient and safe energy will drive the further development of cost-efficient power stations with increasing efficiency coupled with reduced environmental impact [8]. This is a big challenge for the energy conversion technology in the coming decades, that can only be met by a better understanding of high-temperature materials behaviour and by improved design methodologies. The present project, summarized in the following, can be seen only as a first step toward an advanced design concept.

2. Technical Description

The aim of the project was to develop a general approach to describe the heterogeneous deformation of two-phase nickel-base superalloys. Two different materials, SC 16, with about 40% y'- precipitates, and MC2, with 70% y'- precipitates were used to cover a broad industrial sector. The investigations were limited to two temperatures for each alloy, room temperature, and 950°C for SC 16 and 1050°C for MC2, respectively, to study the mechanical behaviour dominated by deformations with and without shearing of precipitates. Four types of loadings were used to perform the tests, uniaxial - , torsion -, tension-torsion - and internal pressure loading. Accompanying microstructural investigations were carried out to study microstructure evolutions.

The partner of the BriteEuRam project 13E.5216 were responsible for

- BAM (project coordinator, model development, mechanical testing and microstructural investigation of SC 16)
- ONERA (model development, mechanical testing of MC2)
- ENSMP (model development, microcstructural investigation of MC2)
- IMMG (development of a torsion-internal pressure testing device, development of measurement techniques for local strain fields, mechanical testing of MC2)

In the following, a short description of the technical details concerning the main research tasks of the research programme is given:

2.1 Prediction of the evolving morphology and the corresponding inelastic deformation (BAM)

External loads and additionally the occurrence of eigenstresses lead to a change of the morphology of the metastable two-phase y/y'- structure of single crystal superalloy. The motion of the y/y' interfaces is driven by diffusion and order-disorder transitions. The energy barriers to be overcome during this motion can be increased or decreased by the local stresses which furthermore prescribe the direction of the diffusion flux. A micromechanical model has been developed which is capable to predict micro-stresses and -strains and the evolving morphology of a single crystal superalloy for various external loadings.

As it was mentioned, the microstructure of γ'-hardened anisotropic single crystalline superalloys is not stable during high temperature loading. For instance under creep loading the alloy SC 16 with [001] orientation formed γ'-platelets perpendicular to the stress axis. This change of the microstructure influences the mechanical properties and the creep strength decreases. One part of the project investigates the single crystalline nickel-base superalloy SC 16 under monotonic, creep, low cycle fatigue and tension/torsion loading at high temperature. After plastic deformation, the microstructure was studied , characterized, discussed, and compared with the mechanical behaviour and with predictions of the model. Under torsional loading the hard and weak zones were investigated by strain field analysis.

2.2 Mechanical behaviour for various morphologies (ONERA)

The work performed at ONERA was devoted to the experimental study as well as to the numerical modelling of the mechanical behaviour of the single crystal superalloy MC2 with

various rafted microstructure. A wide experimental program has been performed at high (1050°C) and low (20°C) temperatures. Test results at 20°C have been used by ENSMP for shear band analysis. At 1050°C most of the loading conditions have induced a coarsening of the microstructure.

Experimental results have shown that the rafting process which occur at high temperature change the mechanical behaviour compared to the initial cuboidal microstructure. It is most important that due to the oriented coalescence of the y'- precipitates there is a loss of the initial cubic symmetry, a decreasing strength of the alloy, and a decreasing Young's modulus. Thus it is essential to take into account the influence of the shape of the y'- precipitates into the constitutive model. The FE calculations of a periodic arranged representative cell, performed in 3D, allow to analyse the internal stress and strain distributions that are due to the misfit strain and to external loading conditions.

2.3 **Strain localization, formation of slip bands and shear bands (ENSMP)**

The formation and propagation of intense slip bands have been observed in SC 16 specimen under tensile loading at low temperature. To predict the occurrence of localized deformation modes in single crystals, we have considered them as bifurcation modes for the non-linear boundary value problem. A bifurcation analysis has been performed for elasto-plastic single crystals undergoing single or multiple slip, which gives a localization criterion and the orientation of the associated shear bands. Since intense slip bands appear at incipient plasticity, a local strain softening behaviour must be introduced to trigger localization.

At high temperature, the deformation of single crystal superalloy is heterogeneous at the microscopic level due to the two phase structure of the material. A constitutive model has been proposed that takes into account the average deformation of each phase over a volume element. Its main advantage is that it is simple enough to be implemented in a FE code for structural calculations for industrial purposes. It resorts on homogenization technique. The model requires geometrical as well as hardening parameters which have been identified forSC16 at 950°C. The anisotropy of the mechanical behaviour can be described with sufficient accuracy if tests for <001> and c 111> oriented crystals are available for the identification process and if both cubic and octahedral slip systems are taken into account. The predictive capabilities of the model have been tested for <001> single crystals with success.

2.4 **Upgrading of high-temperature experimental techniques (IMMG)**

Development of a torsion-internal pressure machine

A new biaxial testing machine has been designed and constructed which is capable of subjecting thin tubular specimens to cyclic torsional loads (maximum load ±500 Nm) and to a constant internal pressure at temperatures reaching 1050°C. Special attention was given to the correct application of the torque, without inducing any axial loads during shearing, and to the free vertical movement of the upper torsion transmitting plate to accommodate the thermal expansion of the specimen during heating. The internal pressure applying system also allows the free axial elongation of the specimen and in addition, the pressure transmitting pistons have been designed to move together thus compressing the pressure medium equally from both ends. In order to minimise the axial heat loss in the specimen, an intermediate grip assembly has been introduced which is made from an advanced austenitic steel and a NIMONIC 105 end coupling onto which the specimen is either threaded or held together by four NIMONIC 115 keys capable to withstand the 1050°C maximum testing temperatures.

Development of a new pressure transmitting medium

The main reason for seeking an alternative pressure transmitting medium was to enable the visual observation of the specimen surface during testing at high temperatures. In addition it was desirable to conduct such tests without the need to construct a safety vessel for the containment of the explosion when the internally pressurised specimen fails. The traditionally used pressure media such as oil and gas cannot be used under such conditions.

Special glass compounds were therefore considered as a replacement pressure medium since they were expected to have low viscosities, in the range of 10^{55} to 10^{6} Poise, in order to satisfy the safety requirement. Extensive literature searches were conducted for candidate glasses and their relevant physical properties, followed by analytic calculations to determine their basicity , since low basicity values give the required inertness in the melt state when in contact with Cr-Ni based alloys. Ultimately borosilicate (B_2O_3-SiO_2) glass mixtures were selected which in addition give the required viscosity values for a wide range of temperature by changing the percentage weight of the two constituents. This selection was also supported by experimental tests which showed that fused B_2O_3 when left in contact with different Cr-Ni based alloys at 950°C gives the same Raman spectra as the original 'untested' B_2O_3. Finally a number of tests were performed in the internal pressure-torsion machine using various Ni/Cr alloys which validated the performance of B_2O_3-SiO_2 as a reliable and safe pressure transmitting medium.

Experimental techniques for the measurement of local strains

In order to measure the local deformation as the hoHow specimen deforms under load, a long distance microscope has been used in conjunction with a specially developed image capturing and processing system. Grids of markers are carefully machined on the surface of the specimen and in addition each marker is 'filled with ceramic adhesive, capable of withstanding temperatures up to 1650°C, in order to enhance its image from the surrounding material. Once the grid is located on the specimen, the image is transferred via a CCD camera to the computer where the position of the markers is calculated and their relative distances computed. This process can be repeated as often as required to provide measurements while the experiment is under way. The distances between the markers are compared to their original values prior to the application of any loading to compute the deformation in the specimen.

The testing at high temperatures, in the range 850-1050° C, prohibited the microscope head remaining in continuous visual contact with the specimen and it was therefore necessary to open by a small amount the furnace when the position of the markers was captured. In addition with the furnace open and temperatures in the range of 700° C, it was still necessary to position in front of the lens a quartz glass for heat protection. Thermocouple measurements have however shown that the thermal gradients generated in the specimen due to the opening of the furnace are negligible. Nevertheless when the furnace is opened under load during testing at 1050°C, it has been observed that the inelastic deformation starts upon reheating from lower temperatures (970°C and upwards) due to the increased time required to reach the 105O"C level. Finally the heat waves within the furnace and the presence of the protective quartz glass, coupled with a ±50μ depth of field in the microscope/camera assembly, have made the focusing of the microscope difficult and have affected the accuracy of the local shear strain measurements, in particular at magnitudes below 2.5%.

Figure 1 summarizes the research activities of the present project under the BriteEuRam programme. The project were supported by SNECMA, TURBOMECA and SIEMENS (KWU).

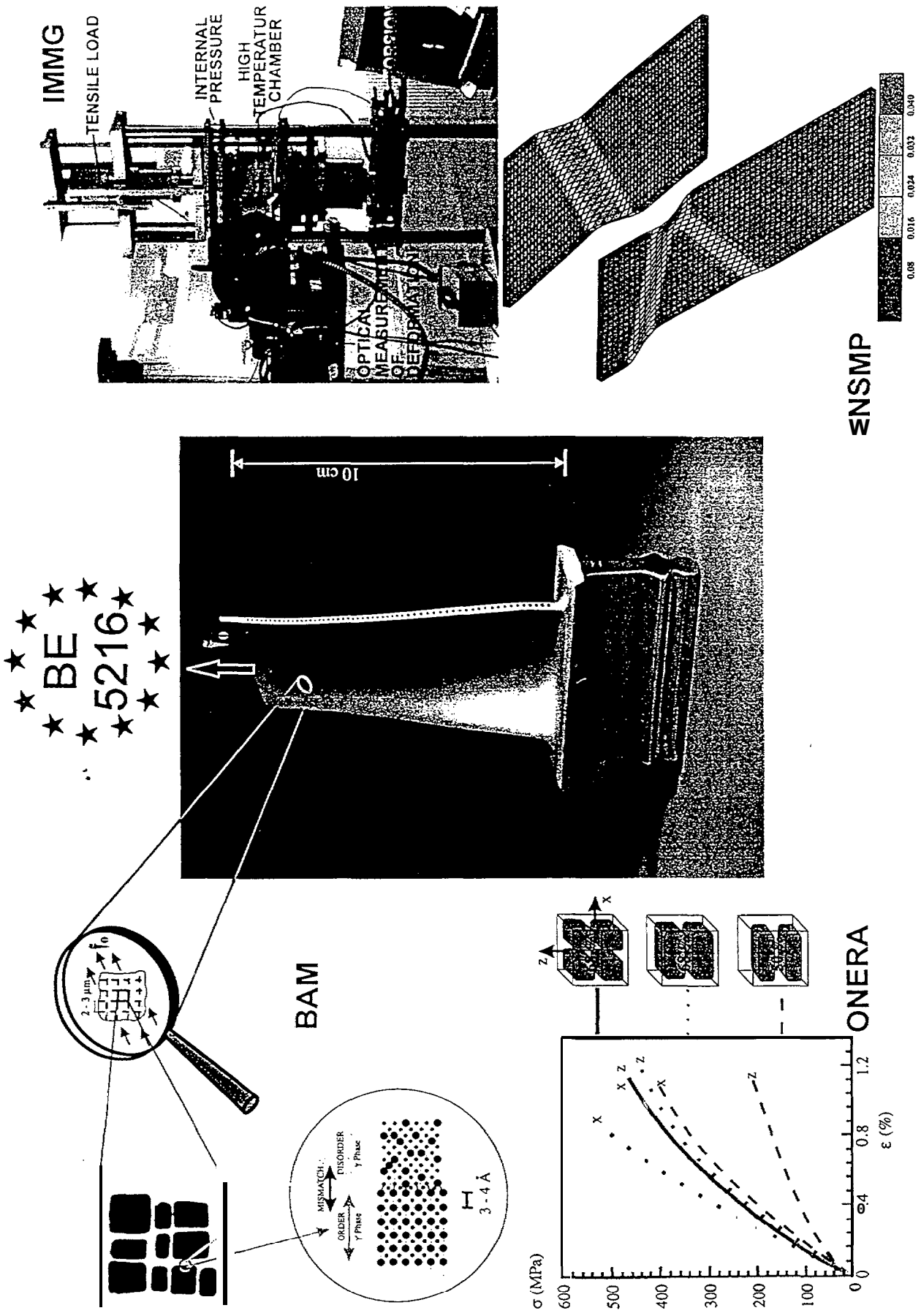

Figure 1: Overview on the research activities of the BriteEuRam projectBE5216.

3. Results

3.1 BAM: Evolving Microstructure of Single Crystal Superalloy

3.1.1 Thermomechanical Modelling

3.1.1.1 Phenomena

In the virginal superalloy the ordered phase, γ', precipitates within the disordered phase, y, resulting in an almost periodic pattern of γ' cuboids. The crystal structure of both phases is face-cubic-centered (fee). However, the lattice parameters of both phases are different which leads to the formation of eigenstresses.

As a consequence of the eigenstresses and the aforementioned loads a change of the morphology of the metastable structure (γ, γ') will occur. The motion of the y/y' interfaces is driven by diffusion and order-disorder transitions. The energy barriers to be overcome during this motion can be increased or decreased by the local stresses which furthermore prescribe the direction of the diffusion flux, [9].

When the microstructure evolves due to an oversaturation of the γ- phase we call this a growth process. The evolution of the microstructure due to a thermal load when there is no oversaturation anymore results usually in a coarsening process, while the change of the microstructure due to mechanical loading leads to the formation of rafts. In case that the (001] crystal axes is parallel to the load axes, the rafts may form parallel or perpendicular to the Ioad axes depending on the sign of the external load and on various material properties as the ratio of stiffness parameters of the phases and the origin of the eigenstrain. In case that *the* load axes deviates from the (001) crystal axes, the growing direction of the rafts are not parallel or perpendicular to the load axes anymore, rather their growing direction follows almost that deviation.

3.1.1.2 The Thermomechanical Model

The most successful existing method to describe the evolution of the morphology by generalized time dependent Landau Ginsburg equations goes back to A.G. Khachaturyan, [10], [11]. The model of the current study belongs to the same class of equations. In this study we model a single crystal superalloy as a body consisting of a binary mixture of alloy elements that may exist in an ordered, (y'), or a disordered, (y), phase. At a given temperature, T, and for given external load, f, we describe the thermomechanical microstate of the body by the fields of strain, concentration of alloy elements and the order parameter. Complete order at stoichiometric composition and complete disorder is characterized by $S = 1$ and by $S = O$, respectively.

A given microstate of the alloy may change due to diffusion and/or order-disorder transition subjected to the local microstress which determines the flow direction. The field equations for these fields rely on the conservation laws of momentum and mass, and on a postulated rate equation for the order parameter.

The BAM model is best suited to predict the evolving microstructure for given external load, [12], [13]. In particular the rafting problem in all its aspects can up to now only be treated by the BAM model. The superiority of the BAM model against existing models is due to its capability to deal with different elastic constants of the y- and y'- phase and to allow an arbitrary

orientation of the crystal axes with respect to the direction of the external load. While the assumption of equal elastic constants in the different phases changes the correct answers to growth and coarsening phenomena only quantitavely, it forbids completely to consider the rafting problem.

3.1.1.3 **Evaluation of the Model and Implementation in a FORTRAN Code**

The BAM model consists of a coupled system of six elliptic equations of second order and six intergral equations of Fredholm type regarding the microstresses and strains, a parobolic equation which is of first order in time and of fourth order in space regarding the concentration of alloy elements, and of a parabolic equation which is also of first order in time and of second order in space regarding the distribution of the alloy elements over the lattice sites.

For the evaluation of this system we have used a discrete Fourier transformation which is applied to a discretized system. This procedure has turn out to be much more effective than the usual Fourier technique, where at first the continuous Fourier transformation is applied to the continuous form of the system and afterwards there is a discretization of the back transformation.

The whole procedure is implemented as a FORTRAN code which consists of a subroutine which computes the stresses and strains for given misfitstrain and given external load, while a second subroutine calls the latter one and computes the resulting morpholgy.

3.1.1.4 The Data Base

Presently, the available date base which is needed as input for the model is not best suited. For example, the different cubic stiffness constants of each phase are still in discussion, because their determination requires a separation of the individual phases, which has first started currently. Another important quantity is the ratio τ_s / τ_c of the relaxation times of order-disorder transitions and of diffusion, respectively. It is generally accepted that order-disorder transitions establishes equilibrium much faster than diffusions] processes. However, it is not certain whether the ratio is 2 or 10, and this value is crucial regarding the constantancy of y'- volume fraction. The BAM model yields an almost constant y'- volume fraction for $\tau_s / \tau_c = 10$ while the y'- volume fraction changes up to 10% for $\tau_s / \tau_c = 2$.

3.1.1.5 Some Results for Special Cases

We shall now illustrate the capability of the model to describe the evolving microstructure by considering various special cases. For all cases we have used the following data: (i) The ratio of relaxation times is $\tau_s / \tau_c = 10$, (ii) The misfit strain depends linearly on the concentration, and is initially positive, (iii)The stiffness coefficients of the phases are related to each other as $c^{\gamma'}_{11} = 0.67 * c^{\gamma}_{11}$, $c^{\gamma'}_{12} = 0.59 * c^{\gamma}_{12}$, $c^{\gamma'}_{44} = 0.58 * c^{\gamma}_{44}$, (iv) The temperature is 950°C.

Example 1:

We consider a process that is realized when the alloy is made from the melt, viz. the transition of the growth period to the coarsening period. To this we start initially with sperical γ'-precipitates which are immersed in a slightly oversaturated y- matrix. The (001) crystal axes points in vertical direction. There is no external mechanical load.

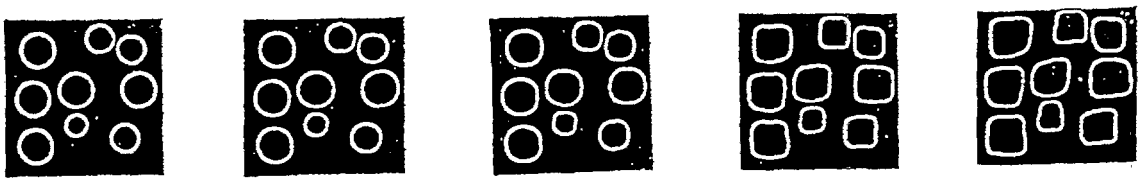

Figure 2: Evolution of morphology under pure thermal load

The sequence of graphs show the evolution of the unstable spheres into cubes which form a more or less periodic array. The final metastable state agrees very we]] with micrographs of real morphologies which were taken after the heat treatments of virginal single crystal superalloy have been finished.

Example 2:

We take the final morphology of Example 1, and expose the alloy in this state to an external mechanical load of 450 MPa which points in vertical direction.

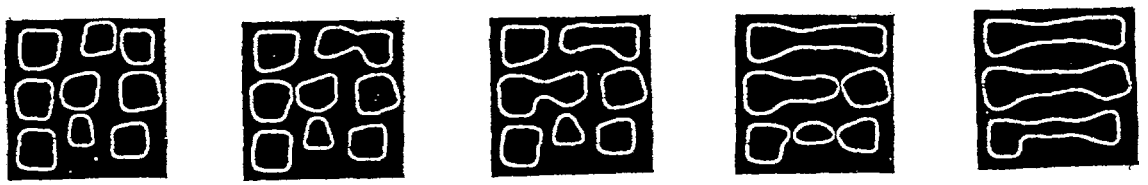

Figure 3: Evolution of morphology under tensile load in vertical direction || (001) crystal axes

The sequence of graphs show the evolution of the well known rafting process. The cubes transform into rafts which are orient themselves perpendicular to the axes of the external load. In the current Bnte Euram project, the simulation of this process has become possible for the first time. It is crucial here to deal with different stiffness coefficients in both phases, because otherwise there is no rafting phenomenon at all. While the coarsening process is more or less the same for equal and for unequal stiffness matrices, the rafting processes appear only if the phases have different stiffness coefficients.

Example 3:

Next we consider the case that the (001) crystal axes deviates from the vertical direction by 12° to the right. At first we consider again the same situation as in Example 1.

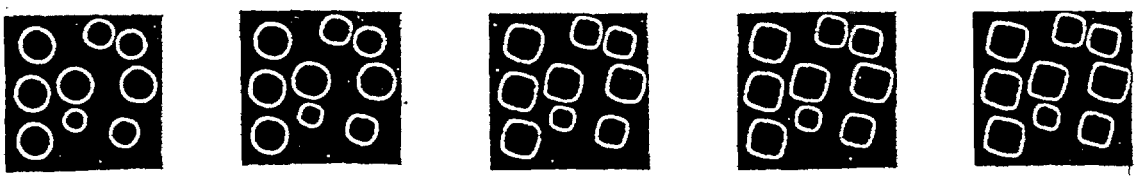

Figure 4: Evolution of morphology under pure thermal load. <(vertical axes, (00 1)crystal axes)= 12°

The sequence of graphs show that obviously the spheres transform into cubes whose axes follow the (001) crystal axes.

Example 4:

Now we take the final morphology of Example 3, and expose the alloy in this state to an external mechanical load of 450 MPa which points again in vertical direction. However, there is now a deviation of 12° between the crystal axes and the axes of the external load.

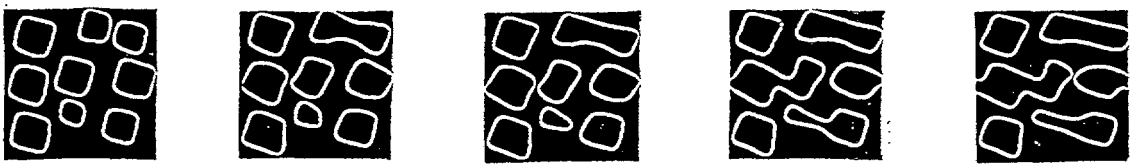

Figure 5: Evolution of morphology under tensile load. <(load axes, (001)crystal axes)= 12°

The sequence of graphs show the formation rafts which are not perpendicular to the axes of the external load anyamore, rather they are almost perpendicular to the (001)crystal axes.

Example 5:

Finally we consider the effect of a compressive load instead of a tensile load. To this we take the final morphology of Example 4, and expose the alloy in this state to an external mechanical compressive load of 450 MPa which points in again vertical direction.

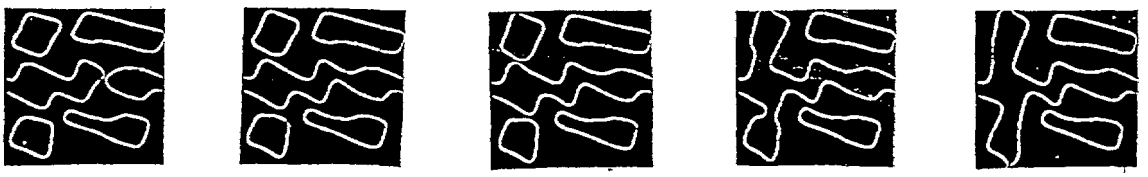

Figure 6: Evolution of morphology under compressive load. <(load axes, (00.)crystal axes)=12°

The sequence of graphs show the tendency to the formation of rafts parallel to the axes of the external load. However, we realize that this is not possible under all circumstances because here there is not enough space for the arrangement of parallel rafts. Only the precipitates on the left hand side can transform to the morphology that corresponds to the new minimum of the free energy.

3.1.2 **Microstructural** observations of the Alloy SC16 Under **Thermomechanical** Loading

3.1.2.1 **Comparison** of **the Microstructure** of the **AS Recieved** Condition with an Annealed Condition **Without** Mechanical Loading

For comparing the microstructure after mechanical loading the as received condition was taken for reference which is shown in Figure 7. The material consists of the y-matrix and the dark cubic γ'-precipitates which have the average size of 45o nm. Additionally small γ'-particles

of 80 nm size are present. After annealing without mechanical loading the microstructure changed. After 1000 hours the big γ'-particles increased and obtained a more round shape and the small precipitates were gone into solution indicating that the microstructure of this alloy is not stable over long time (Figure 8).

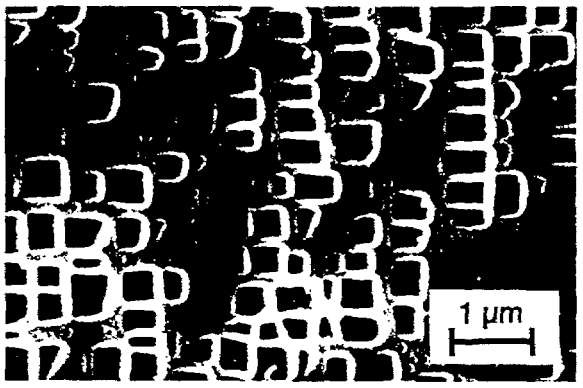

Figure 7: Microstructure of SC 16 in the as received condition

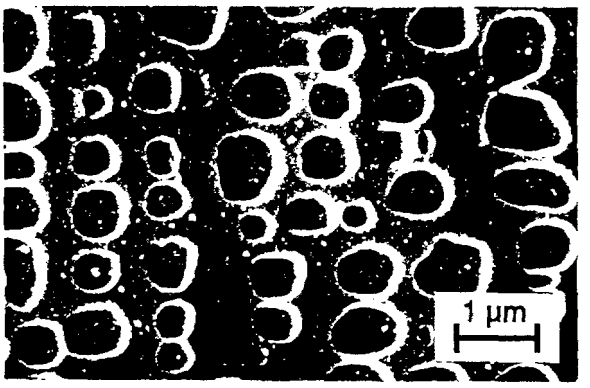

Figure 8: Microstructure of SC 16 after 1000 h annealing at 950°C without mechanical load

3.1.2.2 **Microstructural** Investigations on the **Alloy SC** 16 With Near [001] Orientation After Creep Loading

In Figure 9 the creep strain is shown versus the creep time for tests at 950°C and stress levels of 120 - 200 MPa. With increasing creep load a decreasing time to fracture was observed. During creep deformation a change of the microstructure was observed. It was investigated at different stress levels. A formation of platelets was found which is shown in Figure 9. The platelets were formed perpendicular to the stress axis. At the highest stress level of 200 MPa the specimen reached the lowest time to rupture and the platelets had a fine structure. At low stress levels the time to rupture increased very much and the platelets obtained a more rough shape indicating that the shape of the platelets (rough or fine) is time dependent but not only time dependent. The microstructure of the crepp test with 120 MPa corresponds to a specimen which was not broken. Therefore this figure was not taken for a comparison.

Additionally interrupted tests were performed to investigate the evolution of the microstructure during creep deformation. Figure 10 shows the creep rate versus the creep time. The tests were performed at 950°C and at a creep stress of σ = 135 MPa with testing times of 10 h,100h and 400 h. It was observed that the material shows a hardening until 400 hours. At the same time the microstructure changed. After 10 hours creep time the microstructure in a longitudinal section has not changed very much compared to the as received state. Only the number of small precipitates is reduced but the size and the shape of the big γ'-particles is the same. After 100 hours creep time the development of the platelets perpendicular to the stress axis has been started. The interspace in the vertical direction between γ'-particles was reduced and the precipitates coarsened. The directions perpendicular to the parallel sides of the cubic particles were prefered for coarsening. After 400 hours creep time the progress of the development of Y'- platelets is clearly visible and was almost finished, After 1320 hours creep time the final fracture was observed. The microstructure changed a little and the thickness of the platelets increased and obtained a wavy shape with a mean direction perpendicular to the stress axis.

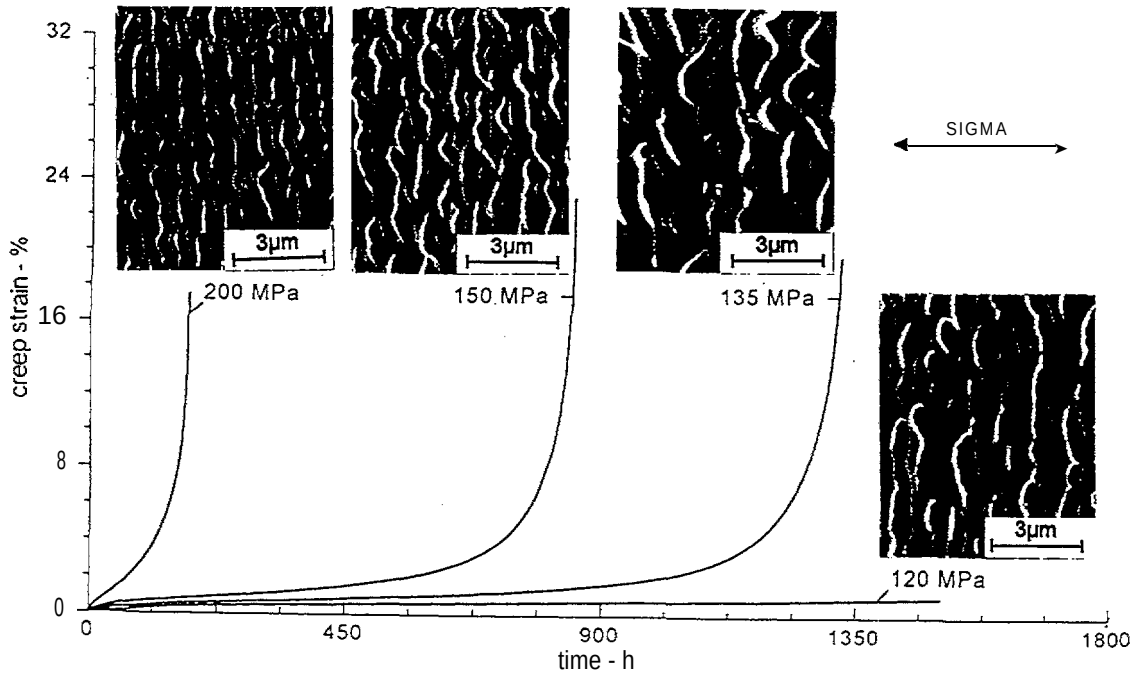

Figure 9: Creep curves of SC 16 with near [001]-orientation at 950°C and the corresponding microstructure after the tests

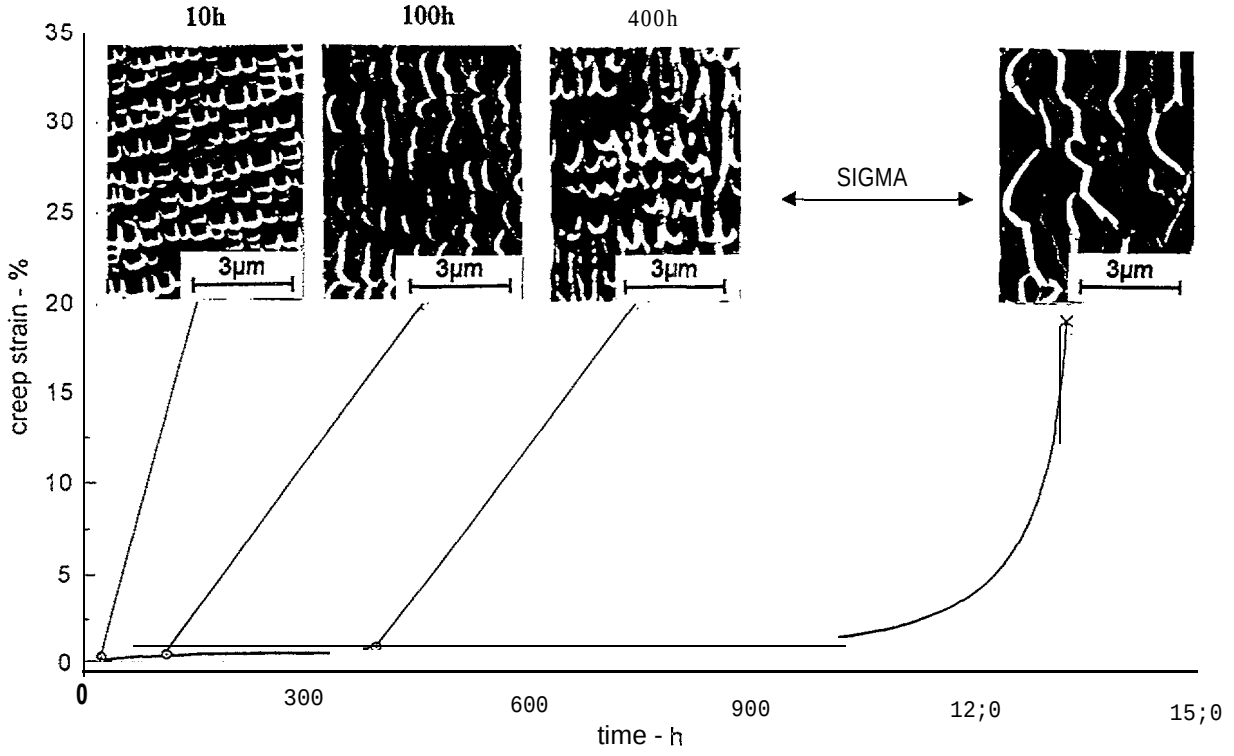

Figure 10: Creep rate versus time of interrupted creep tests at 950°C and 135 MPa creep Ioad of SC 16 with near **[001**]-orientation and the corresponding microstructure after the tests

3.1.2.3 Microstructural Investigations on the Alloy SC 16 With Near [011] Orientation After Creep Loading

After the **creep** tests the specimen developed an elliptic shape of the cross section near the fracture. The elliptic shape and the orientation of the parts of the fracture surface were correlated with crystallographic directions. It was found that the diameter of the specimen was not reduced in the [100] -direction but it decreased specially in the [0$\bar{1}$1]-direction. The fracture surface was observed in a (111)- and ($\bar{1}$1 1)-plane.

The microstructure of a [01 1]-orientated specimen after creep loading is shown in Figure 11. It was found that the platelets were formed in a (001)-plane which was orientated most near perpendicular to the stress axis. The orientation is not equal to the (01 O)-plane because of the deviation (7°) from the ideal orientation of the specimen. Looking to the microstructure in detail we see two competing directions for the formation of platelets:

1. the formation in a (001)-plane but
2. perpendicular to the stress axis some small platelets and y-channels were seen in Figure 11.

Similar results were obtained for a second specimen orientated in the [011]-direction and loaded with 135 MPa.

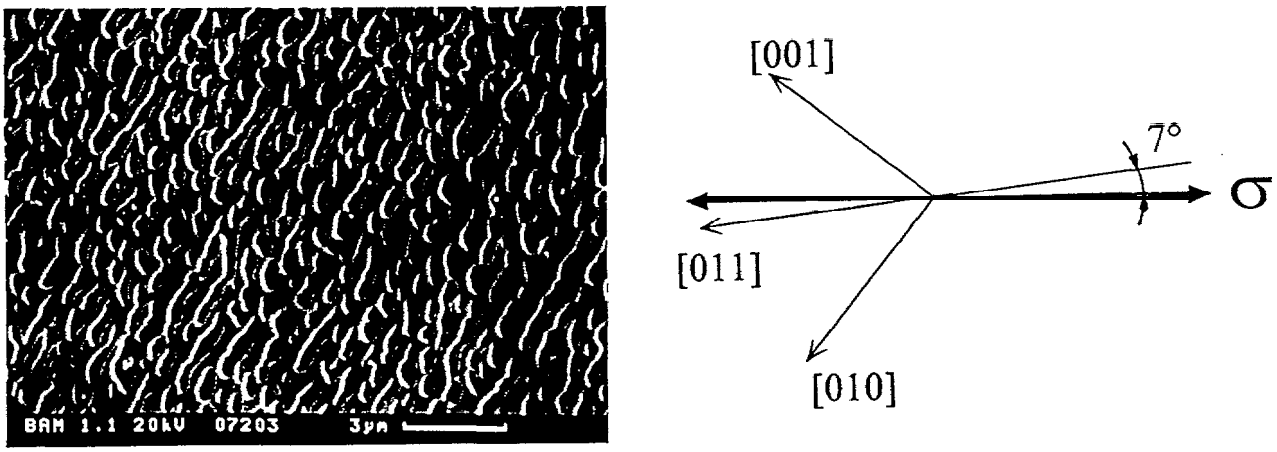

Figure 11: Microstructure of **a** creep test at 950°C of SC 16 with near [011]-orientation

Concluding the observations at creep tests the formation of platelets depends on the interaction of the γ'-particles. They were formed primarily parallel to one of the cubic planes of the γ'-precipitates. The applied stress influences the formation of platelets additionally and it prefers a plane perpendicular to the loading axis. The creep deformation occurs preferential under 45° to the stress axis where the shear stress has a maximum. Therefore it can be explained that the [01 1]-specimen which have built y-channels nearly under 45° to the stress axis failed earlyer than the [001]-specimen that formed y-channels perpendicular to the stress axis.

3.2 ONERA: Constitutive Modelling and Experimental Study of Two Phase Single Crystals

3.2.1 Experimental Study on the Alloy MC2

Two temperatures have been investigated under cyclic tension-compression loading and monotonic torsion, with MC2 specimens oriented along <00 1> and <111> crystallographic orientations. Tests at room temperature were performed for shear band analysis, while high temperature tests (105O"C) were performed for rafting analysis. Some additional tests with prior aging under tension or compression were also performed for that purpose.

In all tests with hold time, or after aging, at high temperature the coarsening of the γ' precipitates is observed. The consequence of this coarsening on the mechanical behavior, for <001> specimens, is a lost of strength of the alloy, when the coarsening is present, compared to the reference behavior on the alloy with an initial cuboidal microstructure. Figure 12 compares the stabilized cycles at a strain rate of 10^{-3} s-[, with and without a prior cyclic loading. For <111> oriented specimens, the effect is not relly observed, excepted for the cyclic test at low strain rate (lO^{-5} s-'), where a cyclic softening is observed for both orientations, starting at the begining of the test. The microstructure generated during this loading conditions, are very different of those obtained at higher strain rate. These differences in the morphologies could explained the softening. An important decreasing of Young's modulus is also observed. These two effects are much more pronounced when the tests are performed at 950°C rather than at 1050°C. Similar effects have been reported in [14],

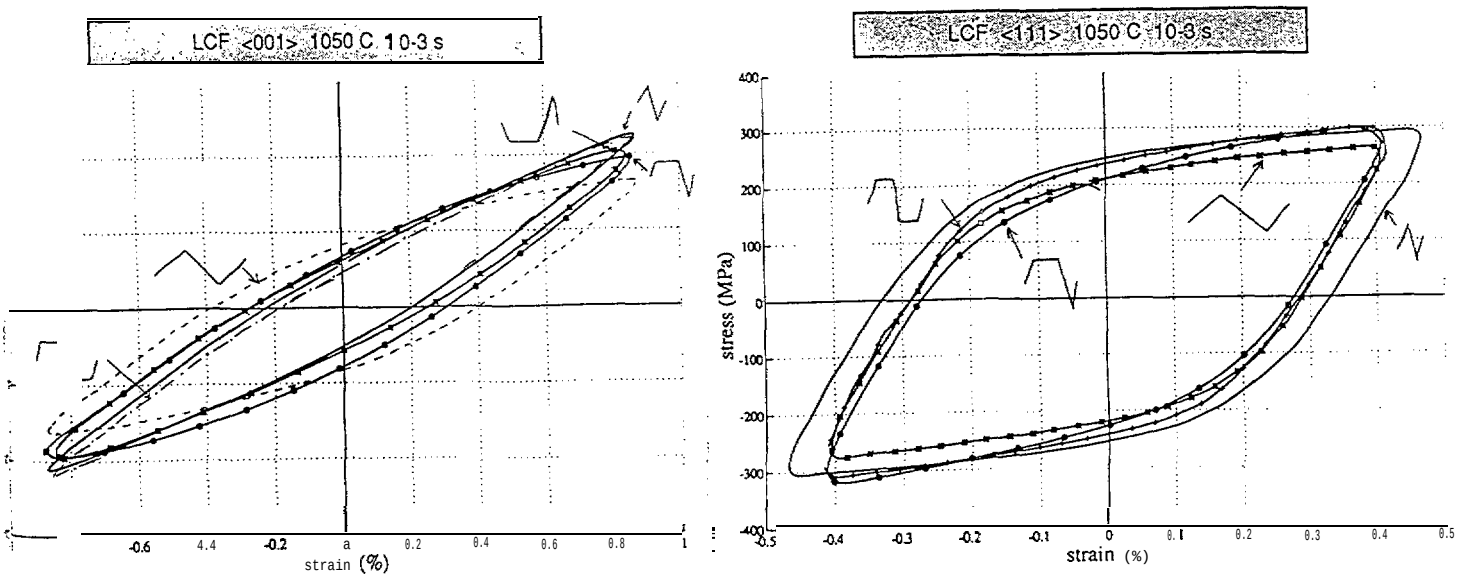

Figure 2 : Effect of prior cyclic loading at 1050°C

3.2.2 Finite Element Calculations of y / y‘ Cells

The coarsening of the y‘ phase of single-crystal superalloy has been widely studied these last years. Some finite element calculations have been used to understand the physical mechanisms, but mainly on the basis of elastic analyses [15,16,17]. In this work, we mainly focused our attention on the influence of the rafted microstructure on the overall behavior of the superalloy. This is done through a 3D Finite Element analysis, taking into account the anisotropic viscoplastic flow of the matrix. A preliminary step is performed, in which the material constants are set for a given discretization of they/ y‘ cell. Results are then discussed at the microscopic level, with the internal stress field analysis due to lattice discrepancy, or due to an external mechanical loading. The overall behavior, deduced from the homogenization calculations is studied, for an initial cuboidal precipitate and for various deformed precipitate morphologies.

The elementary cells considered in this analysis are composed of a cube (initial microstructure) or a parallelepipeds (deformed microstructure) that represents the y‘ phase, surrounded by the matrix channels of y phase. The y‘ volume fraction introduced in the calculation is of 68%, corresponding to the volume fraction of the MC2 alloy that is used in the study to provide the reference macroscopic tensile curves at 105O”C. Periodicity and symmetry conditions are imposed to the boundaries of the cell, so that opposite faces remain planar and parallel during the loading. Cubic elasticity laws are introduced for both phases. The behavior of the y‘ phase is supposed to be elastic, that is a reasonable assumption at high temperature. The anisotropic behavior of the y phase is taken into account through anisotropic viscoplastic models. A macroscopic model and a crystallographic model based on Schmid law have been systematically compared. Both models are strictly equivalent for <001> and <111> orientations [18]. Relations that have been established between the material constants of the two models show that half of the constants of the macroscopical model can be related with octahedral slip, while the other half can be related with cube slip. These relations allow an easy identification of the material constants of the crystallographic model from the macroscopic one. Due to the lack of data on the behavior of the y phase alone, the material constants for the viscoplastic law are obtained by solving the inverse identification problem, through the identification of the macroscopic tensile curve of the y/y’ alloy. In this material, the misfit has a negative value at high temperature, and we have used the data given in the literature: $\delta = -0.3\%$ at 1050°C [16]. A uniform displacement is then imposed on one face of the unit cell, with the same strain rate as in the <001> tensile test. Figure 13 shows the prediction of the macroscopic tensile curve delivered by the finite element calculation. The comparison with the experimental monotonic curve and the first quarter of cycle of cyclic tests is considered as good enough for this preliminary qualitative study.

Due to misfit stresses, the precipitate / matrix coherency requires that the precipitate is initially in tension while the matrix is mostly in compression. Stresses are minimum in the middle of the matrix channels, and maximum near the comers of the precipitate.

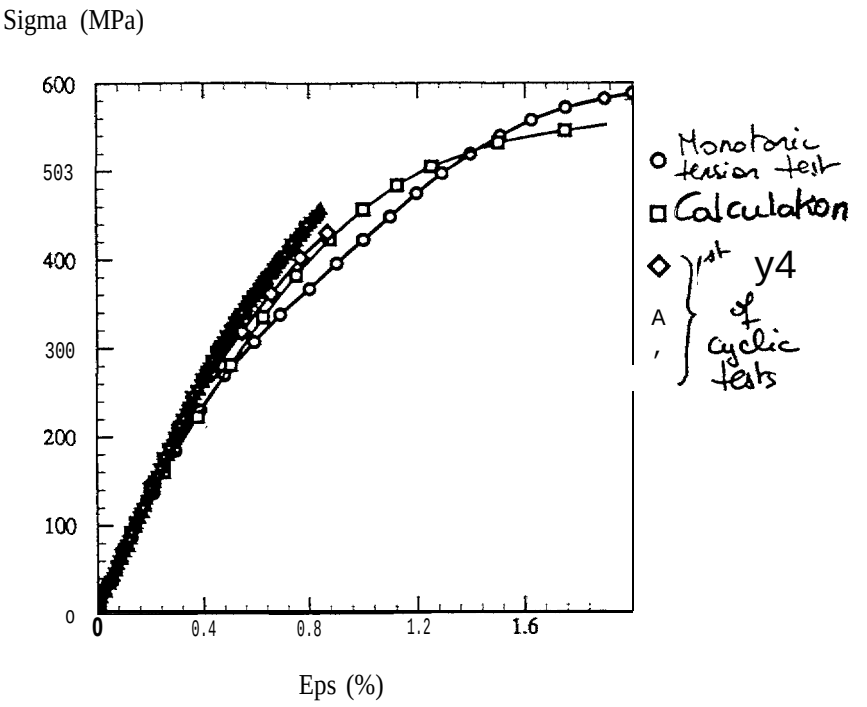

Figure 13: Prediction of the monotonic tensile curve by F.E. calculation

The distribution of von Mises stresses is shown in Figure 14.

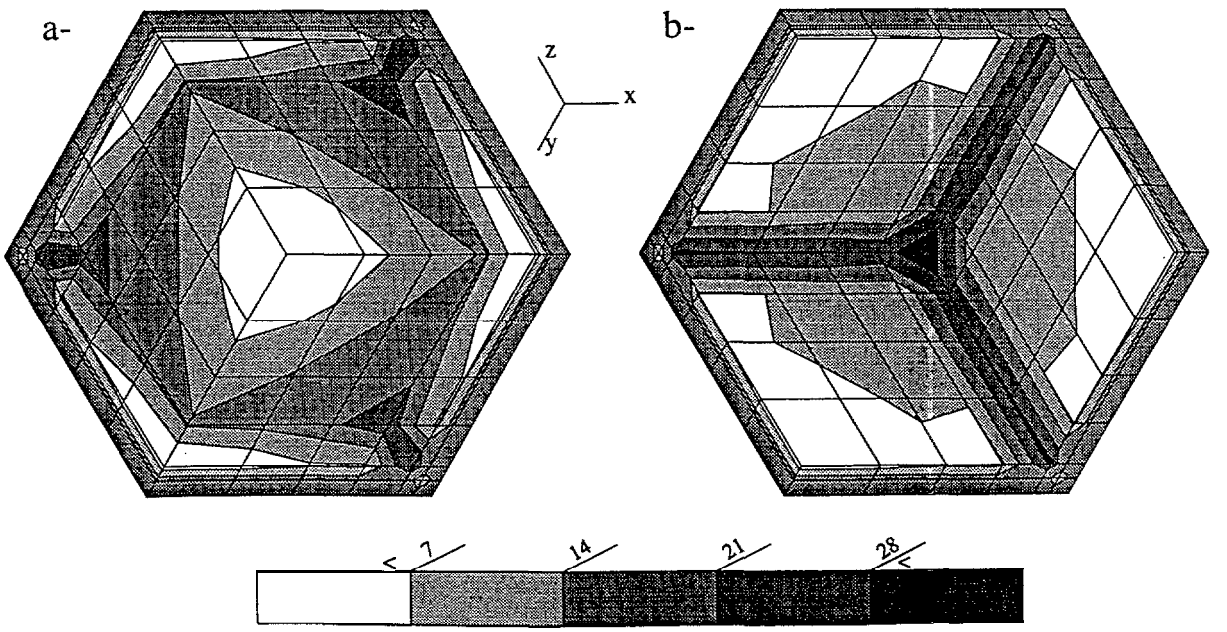

Figure 14: Equivalent von Mises stress contours due to lattice misfit: Within the matrix and the precipitate (a); Only within the matrix (b)

The stress state is mostly triaxial in the matrix channels, the shear stress components are localized in the first row of elements that surrounds the corner of the precipitate. These stresses induce low levels of plastic strains in the matrix. Plastic shear *strains* concentrate along the edges of the precipitate, with a higher intensity however, than the normal strain components. It is worth to note here, that the introduction of the misfit stresses has practically no influence on the resulting tensile curve. The same macroscopic curve is obtained, with and without misfit stresses [19].

At the end of the tensile loading, maximum stresses are obtained in the middle of the matrix channels perpendicular to the loading direction. Shear stresses are still low and limited to the first row of elements, but they are now developed in all the elements that surround the precipitate. A very large plastic flow can be observed in the matrix. The axial component is in tension in all the matrix, except in the middle of the channels perpendicular to the loading direction (intersection of horizontal and vertical matrix channels), where it has a very high negative value. An important strain gradient is developed from the horizontal edges toward the center of cross-channels. After unloading, very small residual stresses are obtained. In the case of cyclic loading, compression loading leads to the same kind of distributions, with inverted signs for stress and strain components.

The calculations were also made with a crystallographic model, using Schmid's criterion. Predictions with both models are almost identical at mesoscopic level (internal stress and strain distributions) and only a small difference is seen at macroscopic level. The crystallographic model provides additional information on the activated slip systems. Cube slip occurs in the first row of elements that surrounds the precipitate, that correspond to the elements where the shear stresses and shear strains localized in the calculations with the macroscopic model.

Several calculations have been performed on various rafted microstructures. Based on microstructurales observations, two typical shapes of precipitates are mainly studied. One is a raft, that is typical of the microstructure generated by a tensile loading, the other one is a rod, typical of the microstructure generated by compressive loading. In all cases, the influence of the microstructure is evaluated through its effect on the macroscopic tensile curve. All the curves are compared to the reference tensile curve, which is provided by the calculation based on a cuboidal precipitate and a y‘ volume fraction of 68%. Several parameters have been studied here, such as the elongation of the precipitate, the depth of the raft or the volume fraction. The influence of the thickness of the horizontal and vertical matrix channels has also been evaluated. It is observed that either an increasing or a decreasing of the strength, compared to the reference situation, can be predict by the calculations, according to the morphology and the loading direction (Figure 15). The volume fraction has a very high effect on the strength of the material. It is also clear that the initial cubic symmetry, characteristic of the material in its initial state, and which is a basic property of the mechanical models developed for these materials, is lost when the coarsening occurs. Figure 16 illustrates the prediction obtained for the morphology schematically represented on the figure, with a horizontal matrix channel much more thicker than the horizontal one. The volume fraction has been reduced down to 50%, that is also more consistent with the measurements made on the same alloy at 1050°C [20].

This F. E. model is then able to provide much information on the mechanical properties, at mesoscopic and macroscopic scales, according to the considered microstructure. This is also an interesting tool, for the development of macroscopic models, taking into account the y and γ' phases, since it can be used as a numerical test machine.

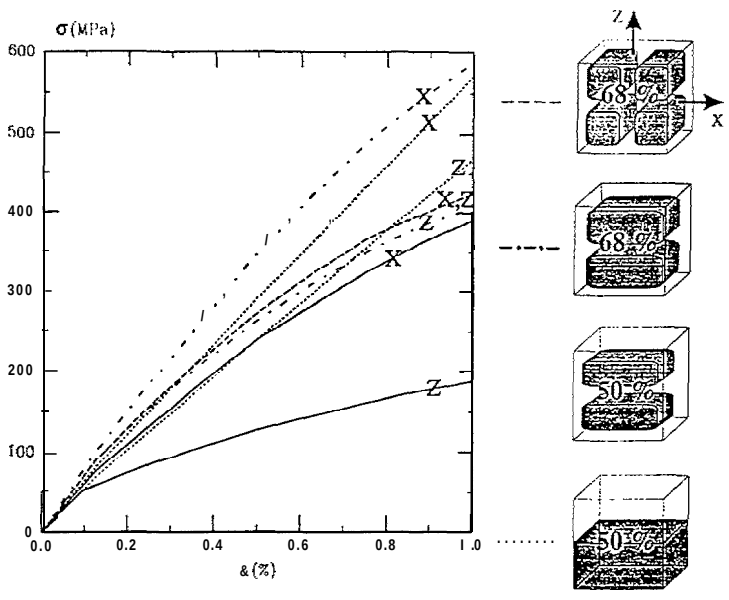

Figure 15: Influence of they' morphology and of the volume fraction

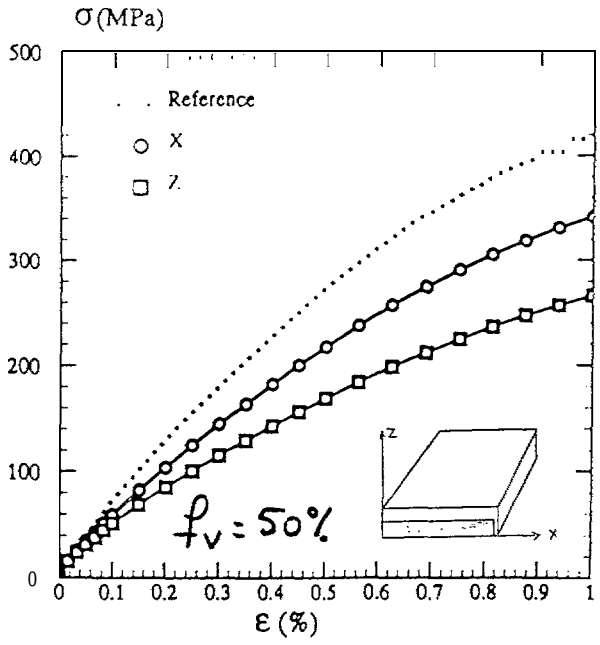

Figure 16: Influence of the channel thickness

3.3 ENSMP: Localized Deformation in Single Crystal Superalloy

3.3.1 Slip Bands, Kink Bands, Shear Bands in F.C.C. Single Crystals

These localized deformation modes in single crystals have been interpreted as bifurcation modes for the non-linear boundary value problem, as done since Hill and Hutchinson [21]. A bifurcation analysis can be performed for single crystals undergoing symmetric multiple slip at small strain. The small strain framework allows us to consider situations for which 4, 6 or 8 are simultaneously activated. In contrast Peirce [22] studied double slip configurations at finite strain. For single slip the slip band and the kink band are equivalent bifurcation modes. Non crystallographic shear band orientations have been found for all other cases [23], For one and four slip systems, bifurcation may occur as soon as the hardening modulus vanishes. In all other cases the theoretical critical hardening modulus is strongly negative so that symmetry-breaking bifurcation modes may develop earlier. The predicted bifurcation modes have been simulated using the FE method within the framework of crystal plasticity. In each case the actual 3D geometry of f.c.c. single crystals has been considered. In contrast most simulations of shear banding in literature make use of Asaro's planar model with 2 or more fictitious slip systems.

3.3.1.1 Local Strain Softening

Asaro arid Rice [24] have proved that bifurcation can occur in single crystals for single slip at finite strain with positive values of the hardening modulus. This is due to local geometrical softening and also non-Schmid effects. However, this becomes possible only after significant straining and coarse slip bands are observed experimentally much earlier. Intense slip bands can appear at incipient plasticity and play a significant role in fatigue. This explains why strain softening must be introduced to trigger localization phenomena at the beginning of plastic flow.

The finite element simulations have then proved that a slip band can nucleate in a zone of local softening and cross surrounding hardening zones or subgrain boundaries and eventuall y the entire cross-section of the specimen. This is accompanied by a serration on the load-displacement curve. The introduction of subsequent hardening after the softening period into the constitutive behaviour leads to the formation of a slip band and the propagation of the localized deformation zone over the entire gauge length of the specimen in a way similar to Piobert-Lüders bands. A naive view of these softening-hardening periods in single crystal behaviour could be the follo wing: once some obstacles for dislocation motion have been freed on some slip planes, deformation localizes in them (softening period); afterwards dislocations are more and more trapped on these planes and this leads to subsequent local hardening. Deformation will then take place in other virgin zones of the specimen.

3.3.1.2 Effect of Latent Hardening

Dislocation interactions are represented in a phenomenological way by the interaction matrix h_{ij}. Strong effects of latent hardening on localization for symmetric double slip have been shown numerically. They can all be explained by the simple relation:

$$k \, \Delta \dot{\gamma} = - Q \, (h_{11} - h_{12}) \, \Delta \gamma$$

where linear viscosity is assumed (coefficient k), A y denotes the difference of slip amount for two slip systems and-Q is a hardening modulus. In particular the usual case and copper crystals for instance, that is $h_{11} < h_{12}$ (latent hardening strictly speaking) leads to stable symmetric double slip configurations in the softening regime. In the formed shear bands both slip systems are simultaneously activated but their orientation is non crystallographic.

3.3.1.3 Effect of Lattice Rotation

The analysis with a formulation of the model at finite strain shows that, even though bifurcation occurs after only small straining, the final simulated bifurcation modes are different whether lattice rotation is taken into account or not. The macroscopic load - displacement curves are very similar for the two cases but, in the case of single slip, the final band can be a slip band or a kink band depending on the location of the defect and on the small or large strain framework. Large amounts of lattice rotation have been detected in the kink bands. An example for the different predictions of the small and the large strain model is shown in Figure 17.

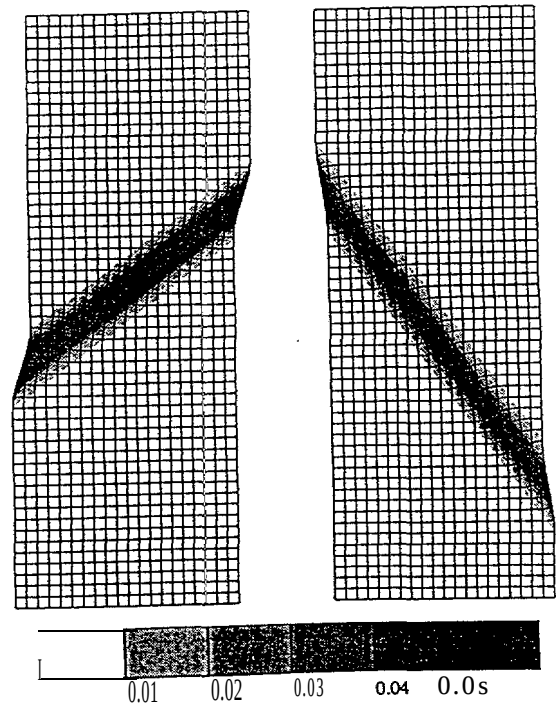

Figure 17: Bifurcation modes obtained with the small (left) and large (right) strain formulation

3.3.2 Description of Lattice Curvature and Torsion Within the Framework of the Mechanics of Generalized Continua

Mandel [25] has laid the basis for a classical treatment of finite deformations of single crystals. Some results of the last section have led us to think that the classical framework is too restrictive to deal with non-homogeneous deformation of single crystals when strong lattice rotation gradients are present. The fact for instance that slip band and king band are equivalent bifurcation modes for single crystals undergoing single slip according. to the analysis at small strains as well as the analysis at finite strains by Asaro and Rice [24], should be regarded as a deficiency of the classical model of crystal plasticity. For slip bands and kink bands are very different physical phenomena observed under different conditions. Contrary to slip bands, kink bands induce strong lattice rotation gradients. The associated strong lattice curvature is accommodated by geometrically necessary dislocations. A more precise description of dislocation populations within the representative volume element should distinguish geometrically necessary dislocations from statistically stored dislocations, The classical hardening variables are related only to scalar dislocation densities measuring the total length of dislocations in the volume element. As for it the continuum theory of dislocations, since Nye [26], considers only the dislocation density tensor which measures the resulting Burgers vector over a volume element. In the present work, we have proposed to incorporate both aspects into the continuum modelling of single crystals. The main feature of the theory is that the description of lattice curvature associated with a non-vanishing dislocation density tensor and of the accompanying couple stresses requires the extension of the continuum to a Coserat continuum (at least).

3.3.2.1 Finite Elastoviscoplasticity of Cosserat Crystals

Recent advances in the mechanics of generalized continua have been used to develop a Cosserat theory for single crystals at finite deformation and curvature. The decomposition of the deformation gradients into elastic and plastic parts is multiplicative as usual, whereas the wryness tensor admits a quasi-additive decomposition. We have assumed that the plastic lattice curvature and torsion are accommodated respectively by edge and screw dislocations belonging to octahedral slip systems in f.c.c. single crystals. The curvature and torsion angles over a characteristic length due to each type of dislocation are internal variables in addition to the amounts of slip for each slip system. The evolution of plastic deformation is due to slip processes:

$$\dot{\mathbf{F}}^{p}\,\mathbf{F}^{p-1} = \sum_{s\in S} \dot{\gamma}^{s}\,\mathbf{m}^{s} \otimes \mathbf{z}^{s}$$

where $\mathbf{m}^s$ is the slip direction for slip system s and $\mathbf{z}^s$ is the normal to the slip plane. The evolution of plastic curvature Γ^p follows

$$\dot{\Gamma}^{p}\,F^{p-1} = \sum_{s\in S} \left(\frac{\dot{\xi}^{s}_{\perp}}{l}\,\xi^{s} \otimes \mathbf{m}^{s} + \frac{\dot{\theta}^{s}_{\odot}}{l}\left(\mathbf{m}^{s} \otimes \mathbf{m}^{s} - \frac{1}{2}\,1 \right) \right)$$

where edge $\perp$ and screw $\odot$ dislocations are taken into account. ξ^s denotes the dislocation line vector. Explicit constitutive equations have been proposed in the case of elastoviscoplasticity.

An important consequence of the theory is that lattice rotation gradients are associated with dissipation. The production of geometrically necessary dislocations is clearly a dissipative process.

3.3.2.2 **Hardening Due to Lattice Curvature and Torsion**

A coupling between plastic curvature and plastic deformation has been introduced at the level of the hardening rule to represent the influence of slip plane curvature on further dislocation motion. Experimental evidence of such hardening effects have been provided in the fifties [27, 28]). An interesting experiment would be to anneal a specimen after twisting and then perform a tensile test again in order to separate the hardening effect of local inhomogeneous lattice torsion from the interaction with stored dislocations belonging to the newly activated slip systems.

The simulation of a torsion test will be an interesting first application of the theory. The determination of material parameters will require additional experimental investigations like simple bending tests followed by tension and torsion tension tests on SC16 single crystals with annealing at larger strains.

3.3.3 Mesh Dependence; Physically Motivated Regularization Methods

Results of calculations performed in a domain in which the uniqueness of the boundary value problem is not ensured must be interpreted with much caution. The predicted post-bifurcation behaviour in such cases is totally mesh-dependent. In particular, in our computations, the load drop (apparition and amplitude) and the post-bifurcation part of the load-displacement curves depend on the type and size of the elements, on the integration and resolution algorithms and on precision. The width of shear bands is also mesh-dependent. In contrast the orientations of the obtained shear band turn out to be mesh-independent. In particular the Localization bands do not coincide with the diagonal of square elements, as claimed sometimes in literature, provided quadratic elements are used. We could reproduce the whole variety of sometimes very peculiar predicted orientations.

3.3.3.1 Role of Viscoplasticity

A complete set of uniqueness and well-posedness theorems and localization criteria, as established in elastoplasticity, is still lacking in the case of viscoplasticity. Our numerical investigations show the pseudo-regularization role played by viscoplasticity. Mesh-dependence turns out to decrease dramatically with increasing viscosity bus the associated Focalization modes become more and more diffuse.

3.3.3.2 Regularization Effects Within the Cosserat Framework

Many regularizing methods have been proposed in the Literature during the last ten years. The use of a Cosserat continuum is one of them. However, they are often used in an *ad hoc* manner without solid physical background. In contrast we have developed our Cosserat theory in order to enrich the description of dislocation distribution at the continuum level and then inspected the possible regularizing capabilities of the model. Regularization can be expected only if a strong coupling exists between lattice curvature and deformation. This is the case for kink bands but not for slip bands.

3.3.4 Between Phenomenology and Micromechanics

Throughout this work we have tried to combine the efficiency of phenomenology with the sound has-is on micro-mechanics and physics. The description of the kinematics of single crystals in both classical and Cosserat cases has its roots in crystallography and dislocation theory, whereas the hardening rules at the slip system level have a phenomenological character. Similarly, in the modelling of two-phase materials, we have adopted the phenomenologically motivated concentration law proposed by Pilvin [29] in order to overcome the tremendous difficulties of self-consistent modelling in elastoviscoplasticity under complex loading paths. Identification methods performed at the macroscopic level and at a more microscopic level, are presented. They require heavy computations but, once the parameters have been determined, they provide explicit constitutive equations that can be used for structural calculations for industrial purposes.

3.3.4.1 Effective Behaviour of Multiphase Materials

The method is based on the choice of one or more representative morphological patterns representing to some extent and in a statistical manner the microstructure of the material. According to the self-consistent scheme, this representative cell is embedded in the infinite unknown homogeneous equivalent medium. Homogeneous or mixed boundary conditions are prescribed at infinity. The corresponding calculations are performed using the FE method. Trial values of parameters characterizing the homogeneous equivalent medium must be chosen and can be some bounds in the elastic case. An optimization process runs then until the mean value of strain over the whole representative cell equals the macroscopic strain prescribed at infinity, up to a certain tolerance. This is the so-called "self-consistency condition". The method provides exact self-consistent estimates in the elastic case.

3.3.4.2 Quasi-Self-Consistent Modelling in the Non-Linear Case

In the non-linear case we have assumed that the form of the constitutive equations for the homogeneous equivalent medium is known. Some parameters intervening in them are then determined using the same optimization procedure as previously, to best fulfill the selfconsistency conditions along some loading paths. If the proposed form of the homogenized constitutive equations is pertinent, this condition will then hold approximately also for other loading paths. This must of course be checked. We have used the following explicit concentration rule in the isotropic case

$$\sigma_i = \Sigma + \mu \left(B - \beta_i \right)$$

with

$$\dot{\beta}_i = \dot{\varepsilon}^p_i - D\, J_2 \left(\dot{\varepsilon}^p_i \right) \beta_i \quad \text{and} \quad \mathbf{B} = \sum_i f_i \beta_i$$

This relation gives the local mean stress in phase i knowing the macroscopic stress Σ and the mean viscoplastic strain $\epsilon^p{}_i$ in each phase. f_i denotes the volume fraction of phase i. We have checked using the FE method that it predicts with enough accuracy the mean stress state in each inclusion of phase i in the cyclic and non-proportional cases, even for elasto-viscoplasticity.

3.3.4.3 Extension to the Anisotropic Case; Behaviour of SC16 at 950 °C

Micromechanical modelling of single crystal nickel-base superalloy is usually based on an assumption of periodicity. In contrast, we have adopted the self-consistent approach which is appropriate mainly for totally disordered phase or pattern distributions. One of the reasons is that the phase distribution is quasi-periodic at the scale of some precipitates (some microns) but no space correlation subsists at the scale of 100 or more precipitates which corresponds to the characteristic size retained for the volume element. The inclusion-matrix morphology has been taken into account via the generalized self consistent scheme. An extension of the previous concentration rule to the anisotropic case is

$$\sigma = \Sigma + \mathbf{C}:(\mathbf{I} - \mathbf{S}):(\mathbf{B} - \beta)$$

where $\mathbf{C}$ is the cubic elasticity tensor and $\mathbf{S}$ the associated Eshelby tensor. The constitutive equation for the two coherent single crystal phases involved isotropic and kinematic hardening variables at the slip system level. The evolution equation are non linear. The material parameters describing each phase must also be determined because the behaviour of each phase within the aggregate is to a large extent unknown. For that purpose experimental data concerning on the one hand the macroscopic response of the material under tension and cyclic loading and, on the other hand, as much microscopic information as possible (local strains, activated slip systems...) must be introduced into the identification procedure. We have distinguished "geometrical" parameters (here parameter D) from materials parameters (viscosity, hardening...): both sets of parameters must be identified simultaneously. The determination of the "geometrical" parameters requires large-scale FE computations over the representative cell embedded in the infinite homogeneous equivalent medium to ensure the fulfillment of the "self-consistency" condition, whereas homogeneous mechanical tests are simulated and compared with experimental results for the identification of the material parameters. A simultaneous identification procedure is necessary because the "geometrical" parameters intervening in the concentration rule depend also on the behaviour of each phase.

Only scarce information on the stress-strain state of each phase during straining was available. The only clear microstructural information is that at high temperature and for low strain rates deformation takes place mainly in the matrix channels. During the identification procedure, constraints have been imposed on the relative critical shear stresses and hardening moduli of the two-phases. A satisfying description of tension and cyclic tests in direction [001] has been obtained. The tensile behaviour in directions [111] and [01 I] is also correctly accounted for, but additional experiments are needed. With the proposed parameters, the model fulfills the "self-consistency" condition for tension tests in directions [001] (identification) and [011] (prediction).

3.3.5 Quantitative Analysis of Localized Deformation

Sophisticated mechanical models accounting for non-homogeneous deformation of materials cannot develop without parallel advances in experimental techniques of local strain measurements. We have shown that strain gauges can be used if the location of strain inhomogenities area *priori* known.

3.3.5S Local Strain Measurements in Non-Uniform Fields

The analysis of tension-torsion tests on SC 16 single crystals at room temperature proves that very complex strain distributions can be detected using a sufficient number of strain gauges. This requires constant exchanges between FE simulation, specimen preparation and final testing. Preliminary calculations are needed to choose carefully the number and location of the strain gauges. The feedback to the model has shown good prediction capabilities of the classical crystal plasticity framework. Tests on [01 1] and [111] specimens are planned and the comparison of local measurements with the FE analysis will be performed. Nevertheless, the use of strain gauges is not well-suited for torsion at larger strains. Furthermore experimental techniques are still lacking to investigate the strain field during torsion at high temperature.

3.3.5.2 Interpretation of Tensile Curves for Single Crystals at Low Temperature

Some common features can be noticed between tensile curves of single crystal nickel-base superalloy at room temperature. The yield point is followed by a small load drop, a plateau and subsequent hardening. We would like to emphasize the fact that such load-displacement curves r-nay well be systematically associated with non-homogeneous deformation of the specimen during testing. Experimental evidence of intense slip band propagation has been shown in the project. A tentative modelling of this phenomenon has been proposed. It is likely that the actual hardening properties of the material can be read on the load-displacement curve only once slip bands have invaded the entire specimen gauge, which corresponds to the subsequent hardening period. A quantitative modelling of slip band propagation could integrate these hardening properties as the intrinsic hardening behaviour of the single crystal, after a short imperceptible local softening transition to trigger localization. However any quantitative analysis of post-bifurcation computations requires the use of a regularizing method as explained previously.

3.4 IMMG: Testing Under Torsion - Internal Pressure Loadings and Techniques for the Measurement of Local Strains

This part of the project is mainly addressed to the design of a combined torsion - internal pressure testing machine and to the development of a high-temperature strain measurement system. For that reason most of the results obtained here are found to be in chapter 2.4 which is devoted to the technical description of the project.

The testing programme on the single crystal superalloy MC2 was not intended to characterize the behaviour of the alloy in detail. The objective was rather to perform selected tests under internal pressure and/or cyclic torsional loadings on tubular specimens which will provide further experimental results on the anisotropic deformation of the alloy using the optical microscope described above and/or suitable extensometry. Certain tests were also taken to failure in order to provide additional information on the failure mechanisms in this alloy. The cyclic torsional loads have either been applied under torque control, at a loading rate of 0..5 Nm/see, or under torsional angle control, at an angular rate of 0.01 °/sec. Two grids of markers were positioned centrally within the gauge length, in the [100] and [1 10] orientations respectively, and in addition an angular extensometer was positioned just outside the gauge length section of the specimen measuring the [100] deformation.

The main results from the MC2 testing programme are summarised in the following paragraphs. All tests were conducted with specimens within 6° to the <100> orientation.

(i) The cyclic torsion, load controlled tests conducted at 850°C and 950°C have shown that the shear strains in the [1 10] grid are significantly higher than those measured in the [100] grid. Such measurements are presented in Figure 1 from a test where the first two cycles were conducted at 850° C while in the two subsequent cycles the temperature was raised to 950° C. The shear strains from the [100] grid also agree closely with those from the [100] extensometer. These measurements therefore confirm the localisation of the deformation in 'softer' [11 O] zones, as found in 'similar' alloys either from R.T. measurements or from observation of the slip traces **[30].**

(ii)The angle controlled cyclic tests conducted at R.T and 105O"C have shown that a stable response is obtained rapidly, within the first couple loading cycles. From the measurements of the [100] extensometer, at the onset of plastic flow the critical resolved shear stresses for cubic slip, in accordance with Schmid's law, were found to be 394 MPa and 56 MPa at R.T. and 1050"C respectively. In the 1050°C test the crack initiated circumferentially within the [1 10] grid zone and it subsequently 'branched' along the axial direction of the specimen.

(iii)A further test was conducted at 1050°C with the objective of ascertaining the burst pressure following the application of an initial torsional pre-loading cycle at 950°C. The internal pressure was raised in stages and ultimately rupture occurred at an internal pressure of 58.9 MPa or equivalently a hoop stress of618 MPa. This compares well with empirical expressions used in pressure vessel design which give a burst pressure of 55 MPa for a U.T.S value for MC2 of 580 MPa at 105O"C. The ruptured MC2 specimen 'opened axially with the slit normal to the [-1 -1 O] orientation.

4. Conclusions

The microstructure of single crystal superalloy is metastable and change due to thermal load as well as to mechanical load. At BAM, the microstructural observations of the alloy SC14 having about 40% y'- volume fraction at 20°C has revealed that thermal loading leads to coarsening processes, in the course of which the y'- precipitates loose their initially cuboidal shape and in particular decrease the curvature of their edges. Mechanical loading leads to directional coalescence of precipitates and to the formation of rafts. In case that the (001) crystal axes is parallel to the load axes, the rafts may form parallel or perpendicular to the load axes depending on the sign of the external load and on various material properties as the ratio of stiffness parameters of the phases and the ongin of the eigenstrain. In case that the load axes deviates from the (00 1) crystal axes, the growing direction of the rafts are not parallel or perpendicular to the load axes anymore, rather their growing direction follows almost that deviation. A change from a tensile load to a compressive load leads to a more or less chaotic change of shape and arrangement of the rafts.

These phenomena have been simulated and predicted by the BAM model that describes the evolving microstructure in the course of time and takes into account diffusion and order-disorder transition under the influence of anisotropic microstresses.

By means of Fast Fourier Transformation a very effective Fortran code has been developed and is implemented on a DEC 3000/500 AXP machine. The code can be used to compute all components of microstresses and microstrains and to simulate the morphology on the micro scale for various choices of material parameters.

Mechanical tests were performed at high temperature on the single crystal nickel base superalloy SC 16 with different crystal orientations. The tests were conducted under monotonic-,

creep-, LCF- and torsional loading. A broad field of experimental parameters were covered to establish a data base which can be used to calibrate constitutive models. A correlation between the high temperature deformation behaviour and the evolving microstructure has been made. To achieve that, microscopical investigations to characterize the microstructure at different stages of the plastic deformation have been carried out. The experimentally observed deformation behaviour has been compared with model predictions. A good agreement between material response and model simulations was observed.

The coarsening of y'- preticipates has been widely studied in the literature, but mainly from a material point of view. The effect of morphology changes on the mechanical properties is not really well understood. Most of the information that can be found in the literature concerns the influence of the microstructure on monotonic loading conditions.

There are no instigations known concerning the influence of an evolving microstructure on the cyclic behaviour. The tests performed in this project at ONERA have shown that the microstructural evolution, occuring at each cycle, induce a decreasing strength of the alloy. These first results are still limited and need further experimental investigations.

The finite element code developed at ONERA can predict the experimentally observed behaviour. For that, one has to be very careful in the individual identification of the matrix and precipitate material behaviour, respectively. Furthermore, it is very important to take the most realistic y'- morphology into account if the matrix law is considered. The assumed elastic law for the precipitates has also great influence on the overall y/y'- behaviour. Actual data are not sufficient and precise measurements are required to improve the predictability of the model. After having the model constants being set, various deformed microstructures can be considered, and the model can be used to study the macroscopic behaviour for various loading directions, in particular those that cannot be simulated in the experiment. This is an essential point, because it has been shown that the initial cubic symmetry is lost when rafting occurs. The realization of such kinds of tests is then indispensable to fit the constants of the appropriate orthorombic symmetry.

Furthermore, the study done at ONERA has shown that macroscopic models for two phase alloys, deduced analytically from microscopic behaviour, are not sufficient to describe the material behaviour in the case a very high volume fraction of precipitates. Here again, further investigations are needed.

Due to the two phase structure of single crystal superalloy the deformation at high temperature is heterogeneous at the microscopic level. A constitutive model that takes into account the individual average deformation in each of both phases and the various slip systems has been developed. The identification of its parameters has been done for the alloy SC16 at 950°C. "For this, <001> and <111> oriented crystals had been used. The resulting predictive capabilities of the model was demonstrated for <001> oriented crystals.

Localized deformation modes, i.e. slip bands, kink bands and shear bands, that may occur in single crystal superalloy, have been interpreted as bifurcation modes that may appear due to the non-linear boundary value problem. Obviously localized deformation modes are accompanied by the phenomenon of local strain softening, which requires a careful numerically study in order to avoid misleading results. The effects of mesh dependence the role of viscoplasticity and other regularization methods have been demonstrated.

Tension-torsion tests at 20°C for the alloy SC 16 exhibited a very complex strain distribution which were investigated by several strain gauges at the specimen. Two important things have turn out: (i) Strain gauges are appropriate only in the small strain range, (2) There is currently no precise method to detect the strain distribution in tension-torsion tests in the high temperature range.

The development of material models and failure criteria for Single Crystal alloys requires their testing under biaxial loadings and also the local measurement of the deformation due to their anisotropic behaviour. The laboratory prototype testing machine developed in this project offers the flexibility of applying combined internal pressure/torsional loadings. In addition, due to the 'safe' use of the borosilicate glasses as the pressure transmitting medium, it offers new possibilities for local strain measurement using a long distance microscope and image analysis techniques. These developments in experimental techniques have been applied to the testing of MC2 in the temperature range of 850-1050° C. These tests have provided further experimental results on the anisotropic deformation of MC2 and in particular the localisation of the deformation in the 'soft' [110] zones. However experimental difficulties, arising primarily by testing at such high temperatures, have affected the accuracy of the local measurements at low strain levels.

5. Acknowledgements

This work was supported by the European Community under Contract No. BRE2-CT92-0176, Project No. BE-52 16, entitled the *"Development of Microstructure Based Viscoplastic Models for an Advanced Design of Single Crystal Hot Section Components"*. The partners of the above mentioned project gratefully acknowledge also the support by their industrial endorsers SNECMA, TURBOMECA and SIEMENS (KWU).

References

[1] G. Härkegaard, The Design Needs for Advanced Gas Turbine Blading, in: *Materials for Advanced Power Engineering, Part Z, 623-639,* D. Coutsouradis et al. (eds.), Kluwer Acad. Publ., 1994.

[2] S.H. Choi and E. Krempl, Viscoplasticity Theory Based on Overstress Applied to the Modelling of Cubic Single Crystal, European Journal of Mechanics, A/Solids 8, 219-*228, 1989.*

[3] A. Bertram and J. Olschewski, Formulation of Anisotropic Linear Viscoelastic Constitutive Laws by a Projection Method, in: *High Temperature Constitutive Modeling - Theory and Application,* A.D. Freed and K.P. Walker (eds.), ASME, AMD-Vol. 121, 129-137, 1991.

[4] D. Nouailhas and A.D. Freed, A Viscoplastic Theory for Anisotropic Materials, ASME Journal of Engineering Materials and Technology 114,97-104, 1992.

[5] E.H. Jordan and K.P. Walker, A Viscoplastic Model for Single Crystals, ASME Journal of Engineering Materials and Technology 114, 19-26, 1992.

[6] L. Merit, P. Poubanne and G. Cailletaud, Single Crystal Modelling for Structural Calculations. Part 1: Model Presentation; Part 2: Finite Element Implementation, ASME Journal of Engineering Materials and Technology 113, 162-182, 1991.

[7] H. Biermann, S. Spangel and H. Mughrabi, Investigation of Local Lattice Parameter Changes in Monocrystalline Nickel-Base Turbine Blades After Service, in: Proceedings 4th European Conference on Advanced Materials and Processes (EUROMAT'95), D255-D260, 1995.

[8] J. H. Horlock, Combined Power Plants - Past, Present, and Future, ASME Journal of Engineering Gas Turbines and Power 117,608-616, 1995.

[9] R.A. MacKay and L.J. Ebert, The Development of y-y' Lamellar Structures in a Nickel Base Superalloy During Elevated Temperature Mechanical Testing", Met. Trans.A, 16A, 1969-1982, 1985.

[10] A.G. Khachturyan, Theory of Structural Transformations in Solids, New York, 1983.

[11] Y. Wang and A.G. Khachaturyan, Shape Instability During Precipitate Growth in Coherent Solids, Acts. metal. mater., 43, 1837-1857, 1995.

[12] W. Dreyer and J. Olschewski, Order-Disorder Transitions Under Load in Single Crystal Superalloy, in: Proceedings of *Solid-Solid Phase Transformations of Materials,* Farmington Penn. USA 17-22 July 1994, W.C. Johnson, J.M. Howe et. al. (eds), 419-424.

[13] W. Dreyer and J. Olschewski, Evolving Microstructure of Single Crystal Superalloy Under External Load, 5th International Workshop on *Computational Modelling of the Mechanical Behaviour of Materials,* RWTH Aachen, November 1995.

[14] M. Pessah-Simonetti., P. Caron. and T. Khan, Journal de Physique IV, Nov. 1993.

[15] U. Glatzel and M. Feller-Kniepmeier, Scripts Metall., Vol. 23, pp. 1839-1844, 1989.

[16] J. F. Ganghoffer, A. Hazotte, S. Denis and A. Simon, Scripts MetalI., Vol. 25, pp. 2491-2496, 1991.

[17] T. M. Pollock and A. S. Argon, Acts Metall. Mater., Vol. 40, N" 1, pp. 1-30, 1992.

[18] D. Nouailhas, J. P. Culié, G. Cailletaud and L. Méric, Eur. J. Mech., A/Solids, 14, no 1, 137, 1995.

[19] D. Nouailhas and G. Cailletaud, Acts Metall. Mater., to appear.

[20] M. Véron, Thèse de doctorat, Institut National Polytechnique de Grenoble, Janvier 1995.

[21] R. Hill and J.W. Hutchinson, Bifurcation phenomena in the plane tension test, J. Mech. Phys. Solids, Vol. 23, pp. 239-264, 1975.

[22] D. Peirce, Shear Band Bifurcation in Ductile Single Crystals, J. Mech. Phys.Solids, Vol. 31, pp. 133-153, 1983.

[23] S. Forest and G. Cailletaud, Strain localization in single crystals: effect of boundaries and interfaces, Eur. J. Mech., A/Solids, Vol. 14, No. 5, pp. 747-771, 1995.

[24] R.J. Asaro and J.R. Rice, Strain Localization in Ductile Single Crystals, J. Mech. Phys. Solids, Vol. 25, pp. 309-338, 1977.

[25] J. Mandel, Plasticité classique viscoplasticité, CISM, Udine, Springer Verlag, 1971.

[26] J.F. Nye, Some geometrical relations in dislocated crystals, J. Mech. Phys. Solids, Vol. 31, No. 2, pp. 133-153, 1983.

[27] J.J. Gilman, Structure and Polygonization of Bent Zinc Monocrystals, Acts MetalI., Vol. 3,277-288, 1955.

[28] B. Jaoul, Influence de la sous-structure de monocristaux d'aluminium sur la forme des courbes de déformation plastique, C. R. Acad. Sci. Paris, T. 242, pp. 2372-2374, 1956.

[29] P. Pilvin, The contribution of Micromechanical approaches to the modelling of inelastic behaviour of polycrystals, Fourth International Conference on Biaxial/Multiaxial Fatigue, May 31- June 3, Paris, 1994.

[30] D. Nouailhas et al., Experimental Study of the Anisotropic Behaviour of the CMSX-2 Single Crystal Superalloy under Tension-Torsion loadings, in: Advances in *Multiaxial Fatigue,* ASTM 1911, ed by D L McDowell and R Ellis, Philadelphia, 1993, pp.244-258.

Bundesanstalt für Materialforschung und -prüfung

Federal Institute for Materials Research and Testing

Institut Fédéral pour la Recherche et l'Essai des Matériaux

Unter den Eichen 87
D-[redacted] 12205 Berlin
✉ D-12200 Berlin

Telefon (030) 8104-0
Telefax (030) 8112029
Telex 183261 bamb d

- *Berichte*
- *Gutachten*
- *Zulassungen*
- *Zertifikate*
- *Tagungspapiere*
- *Prüfungszeugnisse*
- *Prüfstellenanerkennungen*